Hepatocyte-specific IKK-β activation enhances VLDL-triglyceride production in APOE*3-Leiden mice[S]

Janna A. van Diepen,[1],* Man C. Wong,[†] Bruno Guigas,[§] Jasper Bos,* Rinke Stienstra, Leanne Hodson,[††] Steven E. Shoelson,[§§] Jimmy F. P. Berbée,* Patrick C. N. Rensen,* Johannes A. Romijn,* Louis M. Havekes,*˒***˒[†††] and Peter J. Voshol[2]˒***

Departments of General Internal Medicine, Endocrinology and Metabolic Diseases,* Pulmonology,[†] Molecular Cell Biology,[§] and Cardiology,*** Leiden University Medical Center, Leiden, The Netherlands; Department of General Internal Medicine,** Radboud University Medical Center, Nijmegen, The Netherlands; Oxford Centre for Diabetes, Endocrinology and Metabolism,[††] University of Oxford, Churchill Hospital, Oxford, UK; Joslin Diabetes Center and the Department of Medicine,[§§] Harvard Medical School, Boston, MA; and Netherlands Organization for Applied Scientific Research–Biosciences,[†††] Gaubius Laboratory, Leiden, The Netherlands

Abstract Low-grade inflammation in different tissues, including activation of the nuclear factor κB pathway in liver, is involved in metabolic disorders such as type 2 diabetes and cardiovascular diseases (CVDs). In this study, we investigated the relation between chronic hepatocyte-specific overexpression of IκB kinase (IKK)-β and hypertriglyceridemia, an important risk factor for CVD, by evaluating whether activation of IKK-β only in the hepatocyte affects VLDL-triglyceride (TG) metabolism directly. Transgenic overexpression of constitutively active human IKK-β specifically in hepatocytes of hyperlipidemic APOE*3-Leiden mice clearly induced hypertriglyceridemia. Mechanistic in vivo studies revealed that the hypertriglyceridemia was caused by increased hepatic VLDL-TG production rather than a change in plasma VLDL-TG clearance. Studies in primary hepatocytes showed that IKK-β overexpression also enhances TG secretion in vitro, indicating a direct relation between IKK-β activation and TG production within the hepatocyte. Hepatic lipid analysis and hepatic gene expression analysis of pathways involved in lipid metabolism suggested that hepatocyte-specific IKK-β overexpression increases VLDL production not by increased steatosis or decreased FA oxidation, but most likely by carbohydrate-responsive element binding protein-mediated upregulation of *Fas* expression.▪ These findings implicate that specific activation of inflammatory pathways exclusively within hepatocytes induces hypertriglyceridemia. Furthermore, we identify the hepatocytic IKK-β pathway as a possible target to treat hypertriglyceridemia.—van Diepen, J. A., M. C. Wong, B. Guigas, J. Bos, R. Stienstra, L. Hodson, S. E. Shoelson, J. F. P. Berbée, P. C. N. Rensen, J. A. Romijn, L. M. Havekes, and P. J. Voshol. **Hepatocyte-specific IKK-β activation enhances VLDL-triglyceride production in APOE*3-Leiden mice.** *J. Lipid Res.* **2011.** 52: 942–950.

Obesity is associated with diseases such as dyslipidemia, type 2 diabetes, and cardiovascular disease (CVD). The accumulation of lipids in numerous tissues is accompanied by increased inflammatory processes such as macrophage infiltration and production of inflammatory mediators in

Abbreviations: *Abcg5*, ATP-binding cassette sub-family G member 5; *Abcg8*, ATP-binding cassette sub-family G member 8; *Acox1*, acyl-Coenzyme A oxidase 1; apo, apolipoprotein; ChREBP, carbohydrate-responsive element binding protein; *Cidea*, cell death activator CIDE-A; *Cidec*, fat-specific protein FSP27; *Cpt1a*, carnitine palmitoyltransferase 1a; CVD, cardiovascular disease; *Cyclo*, cyclophilin; *Cyp27a1*, cholesterol 27 hydroxylase; *Cyp7a1*, cholesterol 7 alpha hydroxylase; *Cyp8b1*, sterol 12 alpha-hydrolase; *Dgat1*, acyl:diacylglycerol transferase 1; E3L, APOE*3-Leiden; FAME, fatty acid methyl ester; *Fas*, fatty acid synthase; FPLC, fast-performance liquid chromatography; *Gapdh*, glyceraldehyde-3-phosphate dehydrogenase; *Hmgcr*, HMG-CoA reductase; IκB, inhibitor of κB; IKK-β, IκB kinase β; LIKK, liver-specific IKK-β overexpression; *Mttp*, microsomal triglyceride transfer protein; NF-κB, nuclear factor-κB; *Nr1 h3*, liver X receptor alpha; *Nr1 h4*, farnesoid X activated receptor; *Pklr*, liver-type pyruvate kinase; PL, phospholipid; *Plin2*, perilipin 2; *Plin5*, perilipin 5; *Ppara*, peroxisome proliferator activated receptor alpha; *Ppargc1b*, PPAR-gamma coactivator 1-beta; *Srebp-1c*, sterol regulatory element binding protein 1c; TC, total cholesterol; TG, triglyceride; WAT, white adipose tissue; WT, wild-type.

[1] To whom correspondence should be addressed.
   e-mail: J.A.van_Diepen@lumc.nl
[2] Present address of P. J. Voshol: Metabolic Research Laboratories, Institute of Metabolic Science, University of Cambridge, Cambridge, UK.

[S] The online version of this article (available at http://www.jlr.org) contains supplementary data in the form of one table and two figures.

white adipose tissue. In liver, fat accumulation increases the activity of the pro-inflammatory nuclear factor κB (NF-κB), and liver-specific activation of NF-κB induces metabolic disturbances (1, 2).

Hypertriglyceridemia is caused by accumulation of VLDL particles in the plasma as a consequence of changes in lipid metabolism that are associated with obesity. Pro-inflammatory cytokines can cause hypertriglyceridemia (3) and, conversely, suppression of inflammation may reduce hypertriglyceridemia (4) suggesting a direct causal role for inflammatory pathways in the development of hypertriglyceridemia. In fact, administration of lipopolysaccharide (LPS), an inflammatory component of the outer membrane of Gram-negative bacteria, increases plasma triglyceride (TG) levels (5). However, many inflammatory mediators affect multiple tissues, such as muscle, adipose tissue, and liver and, moreover, they can act on multiple cell types including macrophages. The specific contribution of hepatocytes in the relation between inflammation and TG metabolism has never been studied.

In the current study, therefore, we aimed to investigate whether activation of the inflammatory NF-κB pathway exclusively in hepatocytes affects VLDL-TG metabolism and, as a consequence, causes hypertriglyceridemia. To this end, we used hepatocyte-specific transgenic IKK-β (LIKK) mice, which have been described before (1). LIKK mice have an albumin promoter to drive expression of constitutively active human IκB kinase β (IKK-β), which activates the NF-κB pathway selectively in hepatocytes. To study the effects of the hepatocyte-specific inflammation on VLDL-TG metabolism, we crossbred the LIKK mouse with the transgenic APOE*3-Leiden (E3L) mouse that expresses human APOE*3-Leiden (a mutant form of APOE3) and human APOC1 (6), both of which attenuate the clearance of apolipoprotein (apo)E-containing TG-rich lipoproteins. Therefore, the E3L mouse shows increased plasma TG and cholesterol levels and is a well-established model of human-like lipoprotein metabolism (7). By using the E3L.LIKK mouse, we were able to study the effects of the inflammatory NF-κB pathway in the hepatocyte on TG-rich lipoprotein metabolism directly. Our results show that activation of NF-κB in hepatocytes of E3L mice induces hypertriglyceridemia by enhancing VLDL-TG production directly within hepatocytes.

MATERIALS AND METHODS

Animals

LIKK mice, which express constitutively active human IKK-β selectively in hepatocytes under control of the albumin promoter (1), were crossbred with E3L mice (6), expressing both human APOE*3-Leiden and human APOC1, in our animal facility to obtain heterozygous E3L.LIKK mice on a C57Bl/6J background. Male E3L.LIKK and E3L littermates were housed under standard conditions with a 12 h light-dark cycle and were fed a standard mouse chow diet with free access to water. Experiments were performed on 14-week-old animals after an overnight fast. All experiments were approved by the institutional ethical committee on animal care and experimentation.

Western blot analysis

Tissues were homogenized by Ultraturrax (22,000 rpm; 2×5 s) in an ice-cold buffer (pH 7.4) containing 30 mM Tris.HCl, 150 mM NaCl, 10 mM NaF, 1 mM EDTA, 1 mM Na$_3$VO$_4$, 0.5% (v/v) Triton X-100, 1% (v/v) SDS and protease inhibitors (Complete, Roche, Mijdrecht, The Netherlands) at a 1:6 (w/v) ratio. Homogenates were centrifuged (16,000 rpm; 15 min, 4°C) and the protein content of the supernatant was determined using the BCA protein assay kit (Pierce, Rockford, IL). Proteins (20–50 μg) were separated by 7–10% SDS-PAGE followed by transfer to a polyvinylidene fluoride (PVDF) membrane. Membranes were blocked for 1 h at room temperature in Tris-buffered saline with Tween-20 (TBST) with 5% nonfat dry milk followed by an overnight incubation with the following antibodies: p-Ser536 NF-κB p65 (#3031), NF-κB p65 (#3034), p-Ser32/36 IκBα (#9246), IκBα (#9242) (all from Cell Signaling), MTP (#612022) (BD Biosciences, Erembodegem, Belgium), and DGAT1 (#54037) (Abcam, Cambridge, UK). Blots were then incubated with HRP-conjugated secondary antibodies for 1 h at room temperature. Bands were visualized by ECL and quantified using Image J (National Institutes of Health).

Plasma lipids and lipoprotein profiles

Blood was collected from the tail vein into chilled paraoxon (Sigma, St Louis, MO)-coated capillaries to prevent ongoing lipolysis (8). Capillaries were placed on ice, centrifuged, and plasma was assayed for TG, total cholesterol (TC), and phospholipids (PLs) using commercially available enzymatic kits from Roche Molecular Biochemicals (Indianapolis, IN). FFAs were measured using NEFA-C kit from Wako Diagnostics (Instruchemie, Delfzijl, The Netherlands). For the determination of lipid distribution over plasma lipoproteins, Fifty microliters of pooled plasma was used for fast performance liquid chromatography (FPLC). Plasma was injected onto a Superose 6 column (Äkta System; Amersham Pharmacia Biotech, Piscataway, NJ), and eluted at a constant flow rate of 50 μl/min with PBS pH 7.4. TG and TC were measured as described above in collected fractions of 50 μl.

Liver lipids

Lipids were extracted from livers according to a modified protocol from Bligh and Dyer (9). Briefly, a small piece of liver was homogenized in ice-cold methanol. After centrifugation, lipids were extracted by addition of 1,800 μl CH$_3$OH:CHCl$_3$ (3:1 v/v) to 45 μl homogenate. The CHCl$_3$ phase was dried and dissolved in 2% Triton X-100. Hepatic TG and TC concentrations were measured using commercial kits as described earlier. Liver lipids were expressed per mg protein, which was determined using the BCA protein assay kit.

FA composition of liver TG

Liver samples (100 mg) were homogenized with 0.5 ml saline. Subsequently, 5 ml of chloroform-methanol (2:1 by volume) was added containing butylated hydroxytoluene (BHT). In addition, an internal TG standard was added before extraction. Liver lipids were extracted according to the method of Folch et al. (10). Total TG were separated by spotting lipid extracts onto silica gel 60 (Merk) TLC plates and running in hexane-diethyl ether-acetic acid (85:15:1, v/v/v). Lipid bands were visualized under ultraviolet light after spraying with 0.1% ANS (8-anilino-1-naphthalene sulfonic acid), and identified using commercial standards. TG bands were scraped into glass tubes and methylated at 80°C with 1.5% H$_2$SO$_4$ in methanol for 2 h. TG-derived FAs were eluted into hexane. Separation and quantification of the FA methyl esters (FAMEs) from liver TG was achieved using gas chromatogra-

phy on an Agilent 6890 GC (Agilent Technologies, UK) fitted with a 30 m × 0.53 mm (film thickness 1 µm) capillary column (RTX-Wax). Individual FA peaks were identified by a reference containing known FAMEs. FA compositions (mol%) were then determined.

Generation of VLDL-like emulsion particles

VLDL-like TG-rich emulsion particles were prepared and characterized as described previously (11, 12). Lipids (100 mg) at a weight ratio of triolein-egg yolk phosphatidylcholine-lysophosphatidylcholine-cholesteryl oleate-cholesterol of 70:22.7:2.3:3.0:2.0, supplemented with 200 µCi of glycerol tri[9,10(n)-^{3}H]oleate ([^{3}H]TO) were sonicated at 10 µm output using a Soniprep 150 (MSE Scientific Instruments, Crawley, UK). Density gradient ultracentrifugation was used to obtain 80 nm-sized emulsion particles, which were used for subsequent experiments. TG content of the emulsions was measured as described above. Emulsions were stored at 4°C under argon and used within 7 days.

In vivo clearance of VLDL-like emulsion particles

To study the in vivo clearance of the VLDL-like emulsion particles, overnight-fasted mice were anesthetized by intraperitoneal injection of acepromazine (6.25 mg/kg Neurotranq, Alfasan International BV, Weesp, The Netherlands), midazolam (6.25 mg/kg Dormicum, Roche Diagnostics, Mijdrecht, The Netherlands), and fentanyl (0.31 mg/kg Janssen Pharmaceuticals, Tilburg, The Netherlands). Mice were injected (t = 0) via the tail vein with 200 µl of [^{3}H]TO-labeled emulsion particles at a dose of 100 µg of TG per mouse. Blood samples were taken from the tail vein at 1, 2, 5, 10, and 15 min after injection and plasma ^{3}H-activity was counted. Plasma volumes were calculated as 0.04706 × body weight (g) as determined from ^{125}I-BSA clearance studies as described previously (13). After taking the last blood sample, the liver, heart, spleen, muscle, and white adipose tissue (WAT, i.e., gonadal, subcutaneous, and visceral) were collected. Organs were dissolved overnight at 60°C in Tissue Solubilizer (Amersham Biosciences, Rosendaal, The Netherlands) and ^{3}H-activity was counted. Uptake of [^{3}H]TO-derived radioactivity by the organs was calculated from the ^{3}H activity in each organ divided by plasma-specific activity of [^{3}H]TG and expressed per mg wet tissue weight.

In vivo hepatic VLDL-TG and VLDL-apoB production

To measure VLDL production in vivo, mice were fasted overnight and anesthetized as described above. Mice were injected intravenously with Tran^{35}S label (150 µCi/mouse; MP Biomedicals, Eindhoven, The Netherlands) to label newly produced apoB. After 30 min at t = 0 min, Triton WR-1339 (Sigma-Aldrich) was injected intravenously (0.5 mg/g body weight, 10% solution in PBS) to block serum VLDL clearance. Blood samples were drawn before (t = 0) and 15, 30, 60, and 90 min after injection and used for determination of plasma TG concentration as described above. After 120 min, mice were exsanguinated via the retro-orbital plexus and euthanized by cervical dislocation. VLDL was isolated from serum after density gradient ultracentrifugation at d<1.006 g/ml by aspiration (14) and counted for incorporated ^{35}S-activity.

Isolation of primary mouse hepatocytes

Primary hepatocytes were isolated from mouse livers according to the method of Berry and Friend (15) modified by Groen et al. (16). Briefly, the portal vein was cannulated and liver was first perfused with a calcium-free Krebs/bicarbonate buffer saturated with 95% O$_2$ and 5% CO$_2$ at a flow rate of 5 ml/min. Subsequently, perfusion of the liver was continued with calcium-containing Krebs/bicarbonate buffer with 0.0125% collagenase (Roche, Penzberg, Germany) for 10–15 min until cellular disso-

ciation was observed. Cells were gently released and centrifuged four times at 50 g for 1 min at 4°C to remove nonparenchymal cells from pelleted hepatocytes. Isolated hepatocytes were washed and suspended in complete Williams' E medium containing insulin (Actrapid), fetal calf serum, dexamethasone, and penicillin/streptomycin. Hepatocytes were isolated with similar yields from livers of E3L.LIKK and E3L mice, 70–80% viable, as assessed by trypan blue dye exclusion, and 99% free of nonparenchymal cells by visual inspection. No differences with respect to viability were observed between cells isolated from E3L.LIKK and E3L mice. Cells were seeded into 12-well dishes precoated with collagen at a density of $1.0 × 10^6$ viable cells/well in 2 ml complete Williams' E medium. After a 2 h adherence period, nonattached cells were removed from the cultures by careful washing.

In vitro measurement of TG secretion by hepatocytes

TG secretion in vitro was measured as described previously (17). After an overnight incubation, cells were washed two times and incubated 4 h in fetal calf serum-free and hormone-free Williams' E medium. To measure rates of secretion of TG, cells were subsequently incubated in serum-free and hormone-free medium containing 4.4 µCi of [^{3}H]glycerol (Amersham; UK) with or without 0.75 mM oleate (C18:1) complexed with BSA to stimulate lipogenesis. After 1, 2, 4, or 20 h incubation, medium was collected and cells were washed three times and harvested in 2 ml PBS. Lipids were extracted from medium according to a modified protocol from Bligh and Dyer (9, 17). The lipids were dried under nitrogen, dissolved into chloroform with 2 mM tripalmitin added as a carrier and subjected to TLC (Silica gel 60, Merck, Belgium) using hexane-diethylether-acetic acid (80:20:1; v/v/v) as mobile phase. Lipid spots were visualized using iodine vapor and tripalmitin-positive spots were scraped off, dissolved in 0.5 M acetic acid, and assayed for radioactivity by scintillation counting. Protein content of the cells was determined using the BCA protein assay kit as described earlier. Data are expressed as dpm/mg protein.

Hepatic gene expression analysis

Total RNA was extracted from liver tissues using the Nucleospin RNA II kit (Macherey-Nagel, Düren, Germany) according to manufacturer's instructions. RNA quality of each sample was examined by lab-on-a-chip technology using Experion Std Sens analysis kit (Biorad, Hercules, CA). One microgram of total RNA was reverse-transcribed with iScript cDNA synthesis kit (Bio-Rad) and the obtained cDNA was purified with Nucleospin Extract II kit (Macherey-Nagel). Real-time PCR was carried out on the IQ5 PCR machine (Biorad) using the Sensimix SYBR Green RT-PCR mix (Quantace, London, UK). mRNA levels were normalized to mRNA levels of cyclophilin (*Cyclo*) and glyceraldehyde-3-phosphate dehydrogenase (*Gapdh*). Primer sequences are listed in supplementary Table I.

Statistical analysis

Data are presented as means ± SD. Statistical differences were calculated using the Mann-Whitney test for two independent samples with SPSS 16.0 (SPSS Inc., Chicago, IL). $P < 0.05$ was regarded as statistically significant.

RESULTS

LIKK increases liver NF-kB signaling in E3L mice

To verify that LIKK expression in E3L mice increases hepatic NF-κB signaling, livers from E3L and E3L.LIKK mice were assayed for the presence of phosphorylated over total NF-κB and IκBα using Western blot (**Fig. 1**). Indeed,
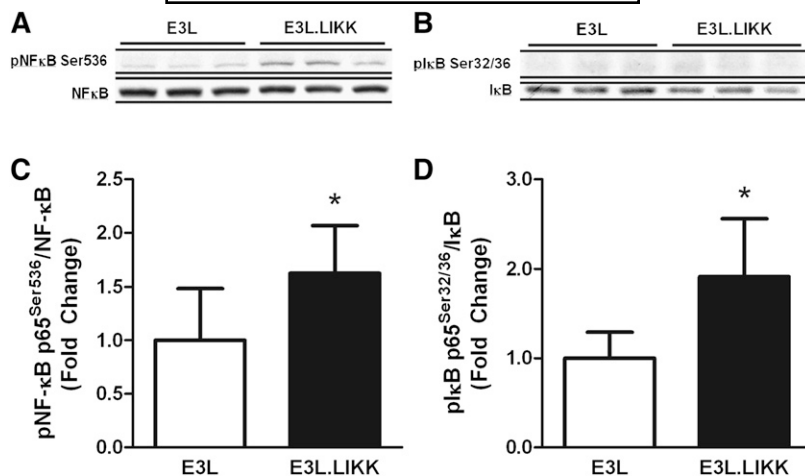
Fig. 1. LIKK increases hepatic NF-κB signaling in E3L mice. E3L and E3L.LIKK mice were fed a chow diet and sacrificed at the age of 14 weeks after an overnight fast. NF-κB signaling was measured in liver tissue by phosphorylation of NF-κB (A, C) and IκB (B, D). Representative Western blots of phosphorylated NF-κB (NF-κB Ser536) and total NF-κB (A) and phosphorylated IκBα (pIκBα Ser32/36) and total IκBα (B) are shown for three mice per group. Ratios of phosphorylated proteins over total proteins were quantified (B, D). Values are means ± SD (n = 5–7). *$P < 0.05$.

expression of LIKK increased the ratio of pNF-κB Ser[536] over NF-κB (1.6 ± 0.4-fold; $P < 0.05$) (Fig. 1A, B) as well as that of pIκBα Ser[32/36] over IκBα (1.9 ± 0.6-fold; $P < 0.05$) (Fig. 1C, D). The increased ratio of pIκBα Ser[32/36] over IκBα was mainly caused by a decrease of total IκBα (0.8 ± 0.1-fold; $P < 0.05$), indicating increased IκBα ubiquitination and degradation by the proteasome, which reflects activation of the NF-κB pathway. These data are in line with the increased NF-κB signaling previously observed in LIKK mice as compared with wild-type (WT) mice (1).

LIKK induces hypertriglyceridemia in E3L mice

To determine whether the hepatocyte-specific inflammation affects plasma lipid levels, TG, TC, PL, and FFA levels were measured in plasma of E3L and E3L.LIKK mice (**Fig. 2**). LIKK expression in E3L mice increased TG by +39% (2.90 ± 0.52 vs. 2.09 ± 0.28 mmol/l; $P < 0.05$; Fig. 2A), TC by +18% (2.24 ± 0.25 vs. 1.90 ± 0.28 mmol/l; $P < 0.05$; Fig. 2B), and PL by +22% (2.12 ± 0.18 vs. 1.74 ± 0.27 mmol/l; $P < 0.05$; Fig. 2C). LIKK did not affect plasma FFA levels (Fig. 2D). Lipoprotein profiling showed that the LIKK-induced increase in plasma TG could be explained by a rise in VLDL-TG (+42%) (Fig. 2E). Likewise, the increase in TC was mainly reflected by an increase in VLDL cholesterol (VLDL-C) (+54%), LDL-C (+34%), and HDL-C (+25%) (Fig. 2F).

LIKK does not affect clearance of VLDL-like emulsion particle-TG in E3L mice

Hypertriglyceridemia is caused by a decrease in VLDL-TG clearance and/or an increase in hepatic VLDL-TG production. To investigate whether LIKK inhibits the clearance of VLDL-TG, the plasma clearance and organ distribution of [³H]TO-labeled TG-rich VLDL-like emulsion particles was evaluated in E3L.LIKK versus E3L mice (**Fig. 3**). LIKK did not affect the plasma half-life of [³H]TO (Fig. 3A), nor the uptake of [³H]TO-derived FAs by

the various organs (Fig. 3B), indicating that LIKK does not increase plasma TG levels by decreasing TG clearance.

LIKK increases VLDL-TG production in E3L mice

As no difference was observed in TG clearance between E3L.LIKK and E3L mice, it is likely that the LIKK-induced increase in plasma TG levels can be explained by an increase of VLDL-TG production. The rate of hepatic VLDL-TG production was measured by determining plasma TG levels after intravenous Triton WR1339 injection (**Fig. 4**). Indeed, LIKK strongly increased the accumulation of plasma TG at all time points (Fig. 4A). The VLDL-TG production rate, as determined from the slope of the curve from all individual mice, was increased by +48% (3.90 ± 1.01 vs. 2.64 ± 0.82 mM/h, $P < 0.05$) (Fig. 4B), whereas the rate of VLDL-apoB production did not change significantly ($P = 0.52$) (Fig. 4C). Because each VLDL particle contains a single apoB molecule, LIKK apparently increases plasma TG levels by enhancing VLDL-TG production without affecting VLDL particle production.

LIKK does not affect liver lipid levels

To investigate whether the increase in hepatic VLDL-TG production was the result of increased lipid substrate availability in the liver, the effect of LIKK on the hepatic lipid content was investigated (**Fig. 5**). However, E3L and E3L.LIKK mice did not differ with respect to liver TG levels (Fig. 5A) and TC levels (Fig. 5B). LIKK did not influence the FA composition of hepatic TG apart from a mild increase in the relative abundance of linoleic acid (18:2 n-6) by +19% ($P < 0.05$) (supplementary Fig. I).

LIKK directly increases TG secretion in hepatocytes from E3L mice

To evaluate whether IKK-β overexpression in hepatocytes directly increases VLDL-TG production, we next studied TG secretion from isolated hepatocytes of E3L
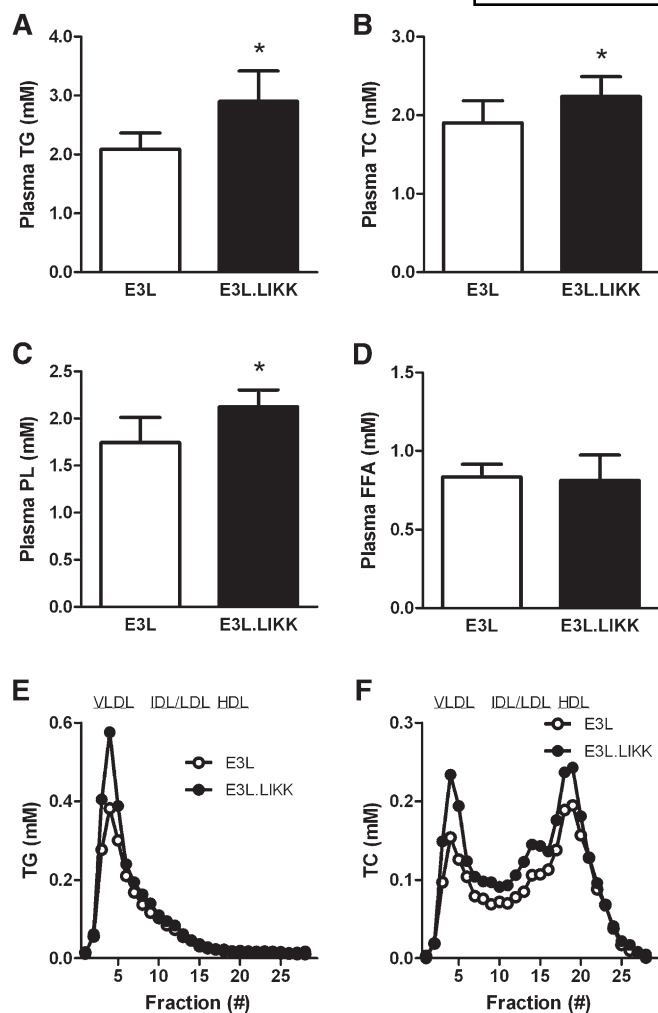
Hepatic inflammation enhances VLDL-TG production 945

Fig. 2. LIKK induces hyperlipidemia in E3L mice. Plasma triglycerides (TG) (A), total cholesterol (TC) (B), phospholipids (PL) (C) and free fatty acid (FFA) (D) levels were measured in plasma of overnight-fasted E3L and E3L.LIKK mice. Values are means ± SD (n = 5–7). *P < 0.05. Plasma was collected, pooled per group, and subjected to FPLC to separate lipoproteins. Distribution of TG (E) and TC (F) over lipoproteins was determined.

Fig. 3. LIKK does not affect clearance of VLDL-like emulsion particle-TG in E3L mice. E3L and E3L.LIKK mice that were fasted overnight were injected with [³H]TO-labeled VLDL-like emulsion particles. Blood was collected at the indicated time points and radioactivity was measured in plasma (A) of E3L mice (open circles) and E3L.LIKK mice (closed circles). Uptake of [³H]TO-derived activity by various organs was determined, and total FA uptake was calculated from the specific activity of TG in plasma and expressed as nmol FA per mg wet tissue weight (B). Values are means ± SD (n = 8). WAT, white adipose tissue; visc, visceral; sc, subcutaneous; gon, gonadal.

and E3L.LIKK mice in vitro. We used [³H]glycerol as precursor for TG synthesis by measuring the accumulation of [³H]TG in the medium (**Fig. 6**). In the absence of oleate, the [³H]TG secretion was low, but LIKK significantly increased the [³H]TG secretion after 20 h of incubation as compared with the [³H]TG secretion from control E3L hepatocytes (2.3-fold; P < 0.05) (Fig. 6A). In the presence of oleate, as a substrate for TG synthesis, [³H]TG secretion was markedly increased, and LIKK caused an additional increase in [³H]TG secretion, reaching significance after 20 h of incubation (1.9-fold at 20 h; P < 0.05) (Fig. 6B).

LIKK increases hepatic expression of FAS but does not affect protein levels or expression of genes involved in VLDL production

To obtain further insight into the mechanism underlying the effects of IKK-β overexpression on VLDL-TG production, we evaluated the hepatic expression of genes involved in VLDL secretion, lipogenesis, FA oxidation,
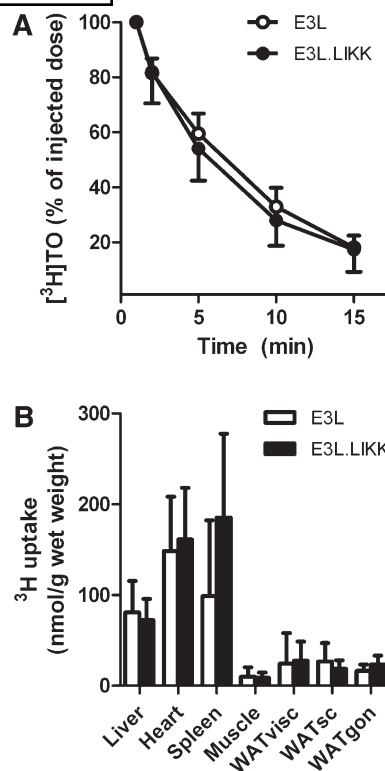
cholesterol metabolism, bile acid metabolism, lipid droplets, and nuclear receptors in livers of E3L and E3L.LIKK mice (**Table 1**). Even though LIKK induced an increase of VLDL-TG production in vivo and in vitro, LIKK did not affect hepatic gene expression or protein level (supplementary Fig. II A, B) of microsomal TG transfer protein (*Mttp*), which is involved in the assembly and secretion of VLDL. In addition, LIKK did not affect apoB (*Apob*) expression, in line with the observation that LIKK did not increase VLDL-apoB secretion in vivo. Also, LIKK did not affect expression of sterol regulatory element binding protein 1c (*Srebp-1c*), which regulates genes required for de novo lipogenesis, nor did it affect expression or protein levels (supplementary Fig. II A, C) of acyl:diacylglycerol transferase 1 (*Dgat1*), which catalyzes the final and only committed step in TG synthesis.

In addition, LIKK did not largely affect clusters of genes involved in FA oxidation [acyl-CoA oxidase 1 (*Acox1*) and carnitine palmitoyltransferase 1a (*Cpt1a*)], cholesterol metabolism [ATP-binding cassette sub-family G member 5 (*Abcg5*), ATP-binding cassette sub-family G member 8 (*Abcg8*), and HMG-CoA reductase (*Hmgcr*)], or bile acid metabolism [cholesterol 7 α hydroxylase (*Cyp7a1*) and ste-
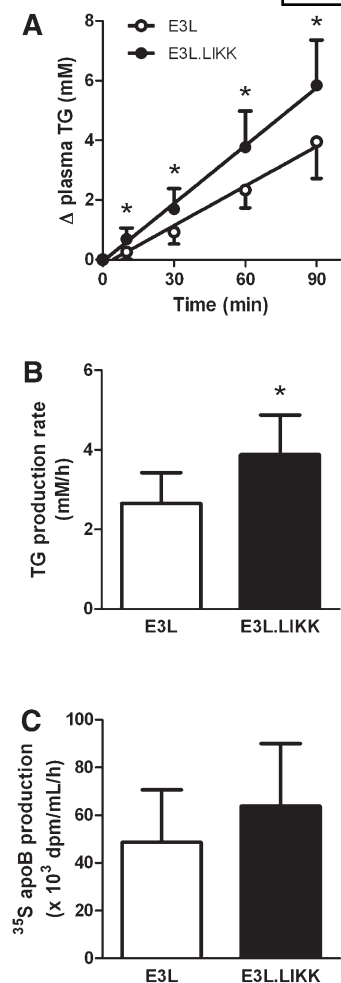
Fig. 4. LIKK increases VLDL-TG production in E3L mice. E3L and E3L.LIKK mice were fasted overnight and injected with Trans^{35}S (t = -30 min) and Triton WR1339 (t = 0) and blood samples were drawn at the indicated time points. TG concentrations were determined in plasma of E3L mice (open circles) and E3L.LIKK mice (closed circles), and plotted as the increase in plasma TG relative to t = 0 (A). The rate of TG production was calculated from the slopes of the curves from the individual mice (B). After 120 min, VLDL was isolated by ultracentrifugation, ^{35}S-activity was counted, and the production rate of newly synthesized VLDL-^{35}S-apoB was determined (C). Values are means ± SD (n = 5–8). *$P < 0.05$.

Fig. 5. LIKK does not affect liver lipid content in E3L mice. Livers were obtained from overnight-fasted E3L and E3L.LIKK mice and lipids were extracted. Triglycerides (TG, A) and total cholesterol (TC, B) concentrations were measured and expressed per mg protein. Values are means ± SD (n = 5–7). *$P < 0.05$.

rol 12 α-hydrolase (*Cyp8b1*)], apart from a 1.9-fold increase in cholesterol 27 hydroxylase (*Cyp27a*) expression. Additionally, LIKK did not affect clusters of genes involved in lipid droplet formation [perilipin 2 (*Plin2*), fat-specific protein FSP27 (*Cidec*), and cell death activator CIDE-A (*Cidea*)] or expression of nuclear receptors [peroxisome proliferator-activated receptor α (*Ppara*), PPAR-γ coactivator 1-β (*Ppargc1*), and liver X receptor α (*Nr1 h3*)], apart from a 1.6-fold increase in expression of perilipin 5 (*Plin5*) and farnesoid X-activated receptor (*Nr1 h4*), respectively.

However, LIKK did increase expression of *Fas*, which plays a key role in FA synthesis, by 2.4-fold, and of liver-type pyruvate kinase (*Pklr*) by 1.7-fold, both of which are target genes of carbohydrate-responsive element binding protein (ChREBP). Taken together, these data suggest that LIK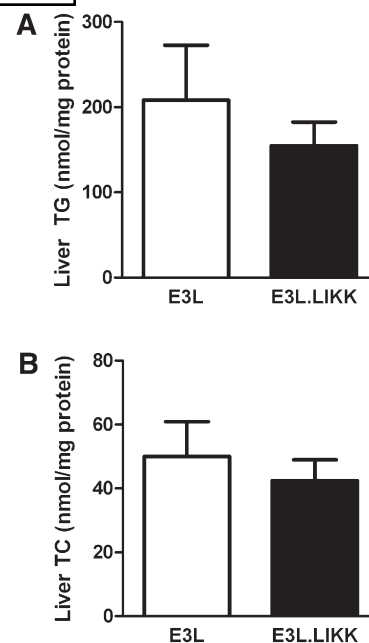K increases VLDL-TG production by ChREBP-mediated upregulation of Fas expression, suggesting an increase in de novo lipogenesis.

DISCUSSION

Obesity leads to an increase in inflammatory processes in numerous organs including the liver (18). In the current study, we questioned whether increased activation of inflammatory pathways in the liver, specifically in hepatocytes, induces hypertriglyceridemia. Indeed, we show that chronic activation of the inflammatory NF-κB pathway specifically in hepatocytes increases plasma TG, which was caused by an increased VLDL-TG production rather than a decreased clearance of VLDL-TG. Furthermore, we provide evidence that the increased TG production induced by hepatocyte-specific IKK-β overexpression is a direct effect of the transgene expression in the hepatocyte.

The strong relation between inflammation and hypertriglyceridemia has largely been derived from the observed increase in plasma TG during acute infection, which is believed to contribute to the host defense (19). However, although similar inflammatory pathways are involved, metabolic inflammation is clearly different from acute inflammation with respect to its cause, intensity, and duration. The inflammation that is observed in obesity is a chronic and low-grade inflammation that is caused by a metabolic overload rather than a pathogen (20). The NF-κB activity in the liver of E3L.LIKK mice in this study is about 1.5-fold higher compared with control E3L mice, which is similar to hepatic NF-κB activation levels seen after high-fat diet feeding and in obesity (1). The present study shows that this low-grade activation of hepatocyte-specific IKK-β in-
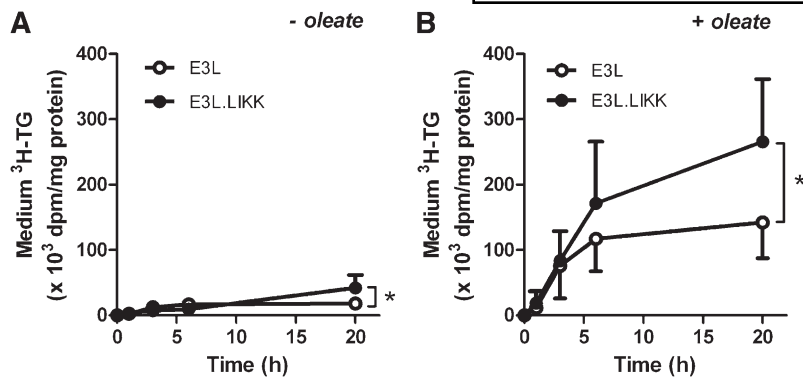
A *- oleate*

B *+ oleate*

Fig. 6. LIKK increases TG secretion in hepatocytes from E3L mice. Hepatocytes were isolated from E3L (open circles) and E3L.LIKK mice (closed circles), cultured overnight, and incubated without or with oleate complexed with BSA. [^{3}H]Glycerol was added to quantify newly synthesized triacylglycerols. Medium was collected at the indicated time points, [^{3}H]TG was measured and expressed as dpm per mg cell protein. Values are means ± SD of 3–6 mice per group, in vitro experiments were performed in triplicate (n = 3–6). *$P < 0.05$.

duces an increase in plasma TG levels in E3L mice, a model for human-like lipoprotein metabolism, which was due to an increase in plasma VLDL-TG levels. Additional investigation of VLDL-TG metabolism revealed that the increased VLDL-TG levels were not caused by decreased clearance of TG from VLDL-like particles, but rather by increased hepatic production of VLDL-TG. These findings are in line with a study showing that injection of a low dose of LPS increases secretion of VLDL-TG, without affecting its clear-ance (5). However, LPS associates with macrophages rather than with hepatocytes (21), which hampers the interpretation of which cell type is primarily responsible for the increase in VLDL-TG secretion. In addition to LPS, individual cytokines that activate various cell types increase VLDL-TG production (3, 22). Because both LPS and cytokines can activate NF-κB signaling, our findings could suggest that the increase in VLDL secretion caused by LPS and cytokines in these earlier studies has been mediated,

TABLE 1. Effect of LIKK on hepatic expression of genes involved in lipid metabolism in E3L mice

Gene	Protein	E3L	E3L.LIKK	Change
VLDL secretion				
Apob	ApoB	1.00 ± 0.35	1.01 ± 0.34	n.s.
Mttp	MTP	1.00 ± 0.46	1.34 ± 0.36	n.s.
Lipogenesis				
Srebp-1c	SREBP1c	1.00 ± 0.39	1.10 ± 0.74	n.s.
Dgat1	DGAT1	1.00 ± 0.32	1.21 ± 0.41	n.s.
Fas	FAS	1.00 ± 0.52	2.43 ± 1.07[b]	+143%
FA oxidation				
Acox1	ACO	1.00 ± 0.70	1.13 ± 0.20	n.s.
Cpt1a	CPT1a	1.00 ± 0.58	0.95 ± 023	n.s.
Glucose metabolism				
Pklr	L-PK	1.00 ± 0.48	1.72 ± 0.80[a]	+72%
Cholesterol metabolism				
Abcg5	ABCG5	1.00 ± 0.22	1.05 ± 0.31	n.s.
Abcg8	ABCG6	1.00 ± 0.16	0.93 ± 0.16	n.s.
Hmgcr	HMG-CoA	1.00 ± 0.19	0.98 ± 0.08	n.s.
Bile acid metabolism				
Cyp7a1	CYP7A1	1.00 ± 0.59	1.19 ± 0.55	n.s.
Cyp8b1	CYP8B1	1.00 ± 0.60	1.21 ± 0.27	n.s.
Cyp27a1	CYP27A1	1.00 ± 0.41	1.85 ± 0.51[b]	+85%
Lipid droplets				
Plin2	PLIN2/ADRP	1.00 ± 0.98	1.04 ± 0.33	n.s.
Plin5	PLIN5/PAT-1	1.00 ± 0.72	1.64 ± 0.55[a]	+64%
Cidec	CIDE-3/FSP27	1.00 ± 0.98	1.05 ± 0.42	n.s.
Cidea	CIDEA	1.00 ± 0.65	0.85 ± 0.59	n.s.
Transcription factors				
Ppara	PPARα	1.00 ± 0.28	0.89 ± 0.16	n.s.
Ppargc1b	PGC-1β	1.00 ± 0.63	0.77 ± 0.26	n.s.
Nr1 h3	LXRα	1.00 ± 0.35	1.09 ± 0.09	n.s.
Nr1 h4	FXR	1.00 ± 0.50	1.58 ± 0.43[a]	+58%

Livers were isolated from overnight-fasted E3L and E3L.LIKK mice. mRNA was isolated and mRNA expression of the indicated genes was quantified by RT-PCR. Data are calculated as fold difference as compared with the control group. Values are means ± SD (n = 8). n.s., not significant. *Abcg5*, ATP-binding cassette sub-family G member 5 ; *Abcg8*, ATP-binding cassette sub-family G member 8; *Acox1*, acyl-CoA oxidase 1; *Apob*, apolipoprotein B; *Cidea*, cell death activator CIDE-A; *Cidec*, fat-specific protein FSP27; *Cpt1a*, carnitine palmitoyltransferase 1a; *Cyp27a1*, cholesterol 27 hydroxylase; *Cyp7a1*, cholesterol 7 α hydroxylase; *Cyp8b1*, sterol 12 α-hydrolase; *Dgat1*, diglyceride acyltransferase 1; *Fas*, fatty acid synthase; *Hmgcr*, HMG-CoA reductase; *Mttp*, microsomal triglyceride transfer protein; *Nr1 h3*, liver X receptor α; *Nr1 h4*, farnesoid X activated receptor; *Pklr*, liver-type pyruvate kinase; *Plin2*, perilipin 2; *Plin5*, perilipin 5; *Ppara*, peroxisome proliferator activated receptor α; *Ppargc1b*, PPAR-γ coactivator 1-β; *Srebp-1c*, sterol-regulatory element binding protein.
[a] $P < 0.05$ compared with the control group.
[b] $P < 0.01$ compared with the control group.

at least in part, via direct or indirect activation of NF-κB in the hepatocytes. In the present study, even though LIKK clearly increased VLDL-TG secretion, there were no significant effects of LIKK on apoB production or hepatic *Apob* gene expression. This suggests that NF-κB activation increases the intracellular lipidation of apoB but not the number of VLDL-particles secreted. This is in contrast with a study by Tsai et al. (23) showing that adenoviral-mediated overexpression of IKK did increase apoB secretion in HepG2 cells. This discrepancy could possibly be explained by the level of IKK overexpression, which was higher with adenoviral-mediated IKK overexpression in their in vitro HepG2 model than with transgenic overexpression in our in vivo study. It is thus reasonable to postulate that low-grade NF-κB activity mainly increases lipidation of the VLDL particles, whereas a higher degree of NF-κB activation could, in addition, increase the number of secreted VLDL-particles.

It is interesting to speculate about the mechanism whereby hepatocyte-specific NF-κB activation increases VLDL-TG secretion, as many different factors could theoretically be involved. For example, IKK-β overexpression can cause insulin resistance (1), which could result in an inability of insulin to suppress VLDL-TG production (24). Furthermore, Kupffer cells have been suggested to play an important role in hepatic lipid metabolism (25). Additionally, Kupffer cell products could possibly suppress lipid oxidation in hepatocytes via NF-κB-mediated suppression of PPARα activity (26). Furthermore, although plasma FFA levels were unaltered by LIKK, liver-directed FA flux may have been influenced, resulting in altered substrate availability for VLDL-TG production. Therefore, to evaluate the effect of IKK-β overexpression in hepatocytes on VLDL-TG production in absence of these potentially confounding factors, we studied the effect of IKK-β in hepatocytes on TG production in vitro. In fact, IKK-β expression in hepatocytes per se appeared to directly increase VLDL-TG production. Although additional factors may contribute to the effect of LIKK on VLDL-TG production in vivo, a direct effect of IKK-β overexpression in hepatocytes thus at least contributes to this phenomenon.

PPAR-α, LXR, and FXR have shown to be activated during inflammation and interact with inflammatory processes (27, 28) and could possibly underlie the mechanism by which hepatocyte-specific NF-κB activation increases VLDL-TG secretion directly within the hepatocyte. However, no change was observed in expression of hepatic PPAR-α and LXR or expression of their target genes. NF-κB activation did increase FXR expression, but FXR activation has been linked to a lower VLDL-TG secretion (29), making a causal relationship between FXR activation and the increase in VLDL-TG secretion unlikely. Apparently, chronic hepatocyte-specific activation of NF-κB by IKK-β overexpression does not induce identical changes in lipogenic pathways that are seen in acute inflammation; however, it clearly increases VLDL-TG production and induces hypertriglyceridemia. Increased hepatic lipid availability, by increased lipogenesis and/or decreased lipid oxidation, could also underlie the mechanism by which hepato-

cyte-specific NF-κB increases VLDL-TG secretion. Acute inflammation has been shown to increase hepatic lipogenesis as measured by incorporation of ^3H_2O into FA in vivo (5, 30, 31). In our study, we measured expression of genes involved in hepatic FA oxidation and de novo lipogenesis. Despite the fact that LIKK did not decrease the expression of genes involved in FA oxidation, LIKK clearly increased expression of *Fas*, which is a key enzyme in the regulation of FA synthesis. Although upregulation of *Fas* could be mediated by the transcription factors LXR, Srebp-1c, and ChREBP (32, 33), the observed upregulation of *Pklr* as a main ChREBP target gene suggests that LIKK most likely activates ChREBP, thereby increasing *Fas* expression. The fact that activation of NF-κB has been linked to local disturbances in glucose metabolism that could activate ChREBP would underscore this observation (1, 34, 35). It is thus conceivable that increased ChREBP-mediated *Fas* expression increases hepatic lipogenesis and thereby increases lipid availability for VLDL-TG production (36). In fact, activation of lipogenesis results in large, but not more, VLDL particles, which is consistent with our findings (37). The fact that we did not observe an increase in the hepatic TG content or FA oxidation that could have been expected by increased *Fas* expression (38) can be explained by efficient incorporation of newly synthesized TG into nascent VLDL resulting in the increased hepatic VLDL-TG secretion.

In conclusion, we show that activation of hepatocyte-specific NF-κB through overexpression of IKK-β increases TG levels in E3L mice by stimulation of VLDL-TG secretion directly within the hepatocyte without effects on VLDL-TG clearance. The stimulation of VLDL-TG secretion is not driven by increased steatosis or decreased FA oxidation, but most likely by ChREBP-mediated upregulation of *Fas* expression.▐▐

REFERENCES

1. Cai, D., M. Yuan, D. F. Frantz, P. A. Melendez, L. Hansen, J. Lee, and S. E. Shoelson. 2005. Local and systemic insulin resistance resulting from hepatic activation of IKK-beta and NF-kappaB. *Nat. Med.* **11:** 183–190.
2. Arkan, M. C., A. L. Hevener, F. R. Greten, S. Maeda, Z. W. Li, J. M. Long, A. Wynshaw-Boris, G. Poli, J. Olefsky, and M. Karin. 2005. IKK-beta links inflammation to obesity-induced insulin resistance. *Nat. Med.* **11:** 191–198.
3. Feingold, K. R., M. Soued, S. Adi, I. Staprans, J. Shigenaga, W. Doerrler, A. Moser, and C. Grunfeld. 1990. Tumor necrosis factor-increased hepatic very-low-density lipoprotein production and increased serum triglyceride levels in diabetic rats. *Diabetes.* **39:** 1569–1574.
4. Goldfine, A. B., R. Silver, W. Aldhahi, D. Cai, E. Tatro, J. Lee, and S. E. Shoelson. 2008. Use of salsalate to target inflammation in the treatment of insulin resistance and type 2 diabetes. *Clin. Transl. Sci.* **1:** 36–43.
5. Feingold, K. R., I. Staprans, R. A. Memon, A. H. Moser, J. K. Shigenaga, W. Doerrler, C. A. Dinarello, and C. Grunfeld. 1992. Endotoxin rapidly induces changes in lipid metabolism that produce hypertriglyceridemia: low doses stimulate hepatic triglyceride production while high doses inhibit clearance. *J. Lipid Res.* **33:** 1765–1776.

6. van den Maagdenberg, A. M., M. H. Hofker, P. J. Krimpenfort, I. de Bruijn, B. J. van Vlijmen, H. van der Boom, L. M. Havekes, and R. R. Frants. 1993. Transgenic mice carrying the apolipoprotein E3-Leiden gene exhibit hyperlipoproteinemia. *J. Biol. Chem.* **268:** 10540–10545.

7. Zadelaar, S., R. Kleemann, L. Verschuren, J. de Vries-van der Weij, J. van der Hoorn, H. M. Princen, and T. Kooistra. 2007. Mouse models for atherosclerosis and pharmaceutical modifiers. *Arterioscler. Thromb. Vasc. Biol.* **27:** 1706–1721.

8. Zambon, A., S. I. Hashimoto, and J. D. Brunzell. 1993. Analysis of techniques to obtain plasma for measurement of levels of free fatty acids. *J. Lipid Res.* **34:** 1021–1028.

9. Bligh, E. G., and W. J. Dyer. 1959. A rapid method of total lipid extraction and purification. *Can. J. Biochem. Physiol.* **37:** 911–917.

10. Folch, J., M. Lees, and G. H. Sloane Stanley. 1957. A simple method for the isolation and purification of total lipides from animal tissues. *J. Biol. Chem.* **226:** 497–509.

11. Rensen, P. C., M. C. van Dijk, E. C. Havenaar, M. K. Bijsterbosch, J. K. Kruijt, and T. J. van Berkel. 1995. Selective liver targeting of antivirals by recombinant chylomicrons–a new therapeutic approach to hepatitis B. *Nat. Med.* **1:** 221–225.

12. Rensen, P. C., N. Herijgers, M. H. Netscher, S. C. Meskers, M. van Eck, and T. J. van Berkel. 1997. Particle size determines the specificity of apolipoprotein E-containing triglyceride-rich emulsions for the LDL receptor versus hepatic remnant receptor in vivo. *J. Lipid Res.* **38:** 1070–1084.

13. Jong, M. C., P. C. Rensen, V. E. Dahlmans, H. van der Boom, T. J. van Berkel, and L. M. Havekes. 2001. Apolipoprotein C-III deficiency accelerates triglyceride hydrolysis by lipoprotein lipase in wild-type and apoE knockout mice. *J. Lipid Res.* **42:** 1578–1585.

14. Redgrave, T. G., D. C. Roberts, and C. E. West. 1975. Separation of plasma lipoproteins by density-gradient ultracentrifugation. *Anal. Biochem.* **65:** 42–49.

15. Berry, M. N., and D. S. Friend. 1969. High-yield preparation of isolated rat liver parenchymal cells: a biochemical and fine structural study. *J. Cell Biol.* **43:** 506–520.

16. Groen, A. K., C. W. van Roermund, R. C. Vervoorn, and J. M. Tager. 1986. Control of gluconeogenesis in rat liver cells. Flux control coefficients of the enzymes in the gluconeogenic pathway in the absence and presence of glucagon. *Biochem. J.* **237:** 379–389.

17. Kuipers, F., M. C. Jong, Y. Lin, M. Eck, R. Havinga, V. Bloks, H. J. Verkade, M. H. Hofker, H. Moshage, T. J. Berkel, et al. 1997. Impaired secretion of very low density lipoprotein-triglycerides by apolipoprotein E- deficient mouse hepatocytes. *J. Clin. Invest.* **100:** 2915–2922.

18. Powell, E. E., J. R. Jonsson, and A. D. Clouston. 2005. Steatosis: cofactor in other liver diseases. *Hepatology.* **42:** 5–13.

19. Khovidhunkit, W., M. S. Kim, R. A. Memon, J. K. Shigenaga, A. H. Moser, K. R. Feingold, and C. Grunfeld. 2004. Effects of infection and inflammation on lipid and lipoprotein metabolism: mechanisms and consequences to the host. *J. Lipid Res.* **45:** 1169–1196.

20. Hotamisligil, G. S. 2006. Inflammation and metabolic disorders. *Nature.* **444:** 860–867.

21. Rensen, P. C., M. Oosten, E. Bilt, M. Eck, J. Kuiper, and T. J. Berkel. 1997. Human recombinant apolipoprotein E redirects lipopolysaccharide from Kupffer cells to liver parenchymal cells in rats in vivo. *J. Clin. Invest.* **99:** 2438–2445.

22. Nonogaki, K., G. M. Fuller, N. L. Fuentes, A. H. Moser, I. Staprans, C. Grunfeld, and K. R. Feingold. 1995. Interleukin-6 stimulates hepatic triglyceride secretion in rats. *Endocrinology.* **136:** 2143–2149.

23. Tsai, J., R. Zhang, W. Qiu, Q. Su, M. Naples, and K. Adeli. 2009. Inflammatory NF-kappaB activation promotes hepatic apolipoprotein B100 secretion: evidence for a link between hepatic inflammation and lipoprotein production. *Am. J. Physiol. Gastrointest. Liver Physiol.* **296:** G1287–G1298.

24. Lewis, G. F., and G. Steiner. 1996. Acute effects of insulin in the control of VLDL production in humans. Implications for the insulin-resistant state. *Diabetes Care.* **19:** 390–393.

25. Huang, W., A. Metlakunta, N. Dedousis, P. Zhang, I. Sipula, J. J. Dube, D. K. Scott, and R. M. O'Doherty. 2010. Depletion of liver Kupffer cells prevents the development of diet-induced hepatic steatosis and insulin resistance. *Diabetes.* **59:** 347–357.

26. Stienstra, R., F. Saudale, C. Duval, S. Keshtkar, J. E. Groener, N. van Rooijen, B. Staels, S. Kersten, and M. Muller. 2010. Kupffer cells promote hepatic steatosis via interleukin-1beta-dependent suppression of peroxisome proliferator-activated receptor alpha activity. *Hepatology.* **51:** 511–522.

27. Glass, C. K., and S. Ogawa. 2006. Combinatorial roles of nuclear receptors in inflammation and immunity. *Nat. Rev. Immunol.* **6:** 44–55.

28. Stienstra, R., S. Mandard, N. S. Tan, W. Wahli, C. Trautwein, T. A. Richardson, E. Lichtenauer-Kaligis, S. Kersten, and M. Muller. 2007. The Interleukin-1 receptor antagonist is a direct target gene of PPARalpha in liver. *J. Hepatol.* **46:** 869–877.

29. Watanabe, M., S. M. Houten, L. Wang, A. Moschetta, D. J. Mangelsdorf, R. A. Heyman, D. D. Moore, and J. Auwerx. 2004. Bile acids lower triglyceride levels via a pathway involving FXR, SHP, and SREBP-1c. *J. Clin. Invest.* **113:** 1408–1418.

30. Feingold, K. R., M. Soued, M. K. Serio, A. H. Moser, C. A. Dinarello, and C. Grunfeld. 1989. Multiple cytokines stimulate hepatic lipid synthesis in vivo. *Endocrinology.* **125:** 267–274.

31. Grunfeld, C., J. A. Verdier, R. Neese, A. H. Moser, and K. R. Feingold. 1988. Mechanisms by which tumor necrosis factor stimulates hepatic fatty acid synthesis in vivo. *J. Lipid Res.* **29:** 1327–1335.

32. Joseph, S. B., B. A. Laffitte, P. H. Patel, M. A. Watson, K. E. Matsukuma, R. Walczak, J. L. Collins, T. F. Osborne, and P. Tontonoz. 2002. Direct and indirect mechanisms for regulation of fatty acid synthase gene expression by liver X receptors. *J. Biol. Chem.* **277:** 11019–11025.

33. Iizuka, K., R. K. Bruick, G. Liang, J. D. Horton, and K. Uyeda. 2004. Deficiency of carbohydrate response element-binding protein (ChREBP) reduces lipogenesis as well as glycolysis. *Proc. Natl. Acad. Sci. USA.* **101:** 7281–7286.

34. Kawaguchi, T., M. Takenoshita, T. Kabashima, and K. Uyeda. 2001. Glucose and cAMP regulate the L-type pyruvate kinase gene by phosphorylation/dephosphorylation of the carbohydrate response element binding protein. *Proc. Natl. Acad. Sci. USA.* **98:** 13710–13715.

35. Yamashita, H., M. Takenoshita, M. Sakurai, R. K. Bruick, W. J. Henzel, W. Shillinglaw, D. Arnot, and K. Uyeda. 2001. A glucose-responsive transcription factor that regulates carbohydrate metabolism in the liver. *Proc. Natl. Acad. Sci. USA.* **98:** 9116–9121.

36. Morral, N., H. J. Edenberg, S. R. Witting, J. Altomonte, T. Chu, and M. Brown. 2007. Effects of glucose metabolism on the regulation of genes of fatty acid synthesis and triglyceride secretion in the liver. *J. Lipid Res.* **48:** 1499–1510.

37. Grefhorst, A., B. M. Elzinga, P. J. Voshol, T. Plosch, T. Kok, V. W. Bloks, F. H. van der Sluijs, L. M. Havekes, J. A. Romijn, H. J. Verkade, et al. 2002. Stimulation of lipogenesis by pharmacological activation of the liver X receptor leads to production of large, triglyceride-rich very low density lipoprotein particles. *J. Biol. Chem.* **277:** 34182–34190.

38. Chakravarthy, M. V., Z. Pan, Y. Zhu, K. Tordjman, J. G. Schneider, T. Coleman, J. Turk, and C. F. Semenkovich. 2005. "New" hepatic fat activates PPARalpha to maintain glucose, lipid, and cholesterol homeostasis. *Cell Metab.* **1:** 309–322.